

Supplemental Itemized List, Gan et al.

Supplemental Itemized List page S1-2

Supplemental Table 1 page S3

This table displays the blood glucose levels before and after exercise in the MCK-PPAR α and MCK-PPAR β mice.

Supplemental Table 2 page S4

This table lists the primers used for the quantitative RT-PCR analysis.

Supplemental Table 3 page S5

This table lists the primers used for the ChIP assays.

Supplemental Figure Legends pages S6-9

Supplemental Figure 1 page S10

This figure demonstrates the gene expression levels seen in the transgenic mice generated for this manuscript, namely the MCK-PPAR β mice. In addition, it outlines the gene expression patterns of the fatty acid oxidation genes in the MCK-PPAR gastrocnemius. Lastly, this figure shows the running distance of the MCK-PPAR mice during a “low-intensity” exercise protocol.

Supplemental Figure 2 page S11

This figure provides a subset of the gene expression profiling data, highlighting the differential regulation of genes involved in muscle glucose metabolism in MCK-PPAR mice.

Supplemental Figure 3 page S12

This figure shows the quantification of the LDH isoenzyme activity gel shown in Figure 1C.

Supplemental Figure 4 page S13

This figure demonstrates that PPAR β binds to a region between -1228 and -1078 of the *Ldhb* gene promoter based on scanning ChIP studies.

Supplemental Figure 5 page S14

This figure demonstrates differential expression of the *Mef2* genes in the MCK-PPAR β vs. MCK-PPAR α muscle.

Supplemental Figure 6 page S15

These data demonstrate increased mitochondrial biogenesis and fatty acid oxidation capacity in the MCK-PPAR mice.

Supplemental Figure 7 page S16

This figure demonstrates that the increase in the LDHB/LDHA ratio increases pyruvate-driven mitochondrial respiration.

Supplemental Figure 8 page S17

These data shows that MCK-PPAR β mice exhibit a greater exercise capacity.

Gan et al._Supplemental Table 1

Supplemental Table 1. Blood glucose levels in MCK-PPAR β and MCK-PPAR α mice

	NTG	MCK-PPAR β	NTG	MCK-PPAR α
Run distance (m)	2086 \pm 201	3559 \pm 186*	1883 \pm 63	1451 \pm 124*
Baseline glucose levels (mg/dL)	153 \pm 8	157 \pm 6	140 \pm 6	168 \pm 10
Post-exercise glucose levels (mg/dL)	72 \pm 13	65 \pm 28	56 \pm 17	365 \pm 34*

Values represent the mean (\pm SEM); n=8-11 mice in each group; * P <0.05 vs NTG

Gan et al._Supplemental Table 2

Supplemental Table 2: RT-PCR primers.

Mouse Gene	Forward	Reverse
36b4	5'-ATCCCTGACGCACCGCCGTGA	5'-GCATCTGCTTGGAGCCCACGT
PPAR β	5'-TCACCGGCAAGTCCAGCCA	5'-ACACCAGGCCCTTCTCTGCCT
PPAR α	5'-ACTACGGAGTTCACGCATGTG	5'-TTGTCGTACACCAGCTTCAGC
Ldhb	5'-AGTCTCCCGTGCATCCTCAA	5'-AGGGTGTCCGCACTCTTCCT
Ldha	5'-TGCCTACGAGGTGATCAAGCT	5'-GCACCCGCCTAAGGTTCTTC
Ucp3	5'-TGCTGAGATGGTGACCTACGA	5'-CAAAGGCAGAGACAAAGTGA
Mef2a	5'-CTACGAGTGGCCATTCCCC	5'-CCAATTCCTCTTCCTCCGAAA
Mef2c	5'-CCTGCTGGTCTCACCTGGTAA	5'-GAACGCGGAGATCTGGCTTA
Mef2d	5'-CCCAGTCTACCCACTCGCTC	5'-GTTGTAGGCAGTGGGCATGG
Slc2a4 (GLUT4)	5'-ATCATCCGGAACCTGGAGG	5'-GTCAGACACATCAGCCCAGC
Cycs	5'-ACCAAATCTCCACGGTCTGTT	5'-GGATTCTCCAAATACTCCATCAG
Cox4i1	5'-TACTTCGGTGTGCCTTCGA	5'-TGACATGGGCCACATCAG
Primers for quantification of mtDNA		
NADH dehydrogenase Subunit 1	5'-CCCATTGCGGTTATCTT	5'-AAGTTGATCGTAACGGAAGC
Lipoprotein Lipase (Lpl)	5'-GATGGACGGTAAGAGTGATTC	5'-ATCCAAGGGTAGCAGACAGGT

Gan et al._Supplemental Table 3

Supplemental Table 3: ChIP primers.

Promoter	Forward	Reverse
Ldhb -181	5'-ACACTCCAGCCTTGTCTTGAAGG	5'-TCCAGCCTCCTAGCTTTCTCCATTG
Ldhb -760	5'-CTCAGCGACTCCTAGGGAAGTTACATC	5'-CACAGTTCCTCCAGGAAACTGCAAG
Ldhb -1228	5'-ACCCAGACTCCCCCAAATTT	5'-TCTTTAAGTGTGTACCTCTTGTCAACG
Ldhb -1807	5'-CTCAGAGACCTGCCTGTTGTC	5'-TGGCTCGTGCCCTTAGTC
Ldhb -3108	5'-TCTAGAGCATAGCACAAACCAGTC	5'-AGAGGTCAGGTCACACTGAGG
Cpt1b PPRE	5'-ACTGTCAACCTTGAGCCCTGGAATTAG	5'-TTGCATCAGTCCTAAAAATAGCTGAATGTA
Ucp1 PPRE	5'-AGTGAAGCTTGCTGTCACTC	5'-GTCTGAGGAAAGGGTTGACC
L32	5'-ACATTTGCCCTGAATGTGGT	5'-ATCCTCTTGCCCTGACCTT

Supplemental Figure 1. Generation of muscle-specific activation of PPAR β

transgenic mice. (A) Northern (top) and Western (bottom) blots showing levels of PPAR β (low (LE), medium (ME), and high (HE) overexpressing lines) in MCK-PPAR β gastrocnemius muscle. A non-specific (N.S.) band is shown as a control for loading. (B) Bar graph demonstrates relative levels of PPAR β mRNA transcript across several tissues in MCK-PPAR β (HE) mice confirming high level expression in skeletal muscle (SKM; gastrocnemius muscle). (C) Heat maps generated from GenMAPP depicting a subset of gene expression array data generated from gastrocnemius muscle of MCK-PPAR α and PPAR β compared to littermate controls. Individual genes involved in fatty acid oxidation (many of which are known PPAR targets) are shown to be regulated in the MCK-PPAR lines as denoted by the color scheme (relative fold change compared to littermate control shown to the right of each gene). (D) Representative Northern blot confirming activation of known PPAR α target genes in MCK-PPAR β gastrocnemius muscle compared to NTG controls; medium chain acyl-Coenzyme A dehydrogenase (*Acadm*), very long chain acyl-Coenzyme A dehydrogenase (*Acadvl*), acyl-CoA thioesterase 2 (*Acot2*), pyruvate dehydrogenase kinase, isoenzyme 4 (*Pdk4*), and acyl-Coenzyme A oxidase 1 (*Acox1*). *36b4* is shown as a loading control. (E) Bars represent mean running distance (\pm SEM) for 12-week-old male MCK-PPAR β and MCK-PPAR α mice and littermate controls (NTG) during low intensity exercise (endurance) protocols (described in Methods) on a motorized treadmill. (Top) Schematic depicts the speed changes over time. n = 8-11 mice in each group. * $P < 0.05$ vs NTG.

Supplemental Figure 2. Differential regulation of genes involved in muscle glucose metabolism in MCK-PPAR β and MCK-PPAR α mice. Heat maps generated from GenMAPP depicting a subset of genes within the expression array dataset generated from muscle of MCK-PPAR α and PPAR β compared to littermate controls. Individual genes involved in glycolysis are shown to be regulated in the MCK-PPAR lines as denoted by the color scheme (relative fold change compared to littermate control shown to the right of each gene). The pathways include glycolysis, lactate/pyruvate metabolism, and glucose oxidation. Of particular interest was the differential regulation of *Ldh2* (*Ldhb*) across the two transgenic lines denoted by the box.

Supplemental Figure 3. Quantification of LDH isoenzyme activity gel electrophoresis (from Figure 1C). Values represent mean % (\pm SEM) total LDH activity. $n \geq 3$ mice in each group. $*P < 0.05$ vs NTG. Note the shift toward the LDHB-containing isoenzymes LDH4, LDH3, and LDH2 with a concomitant drop in LDH5 (lacks LDHB) in skeletal muscle of MCK-PPAR β mice.

Supplemental Figure 4. PPAR β binds to a region within -1228/-1078 of the *Ldhb* gene promoter region. ChIP assays were performed with anti-PPAR β and IgG control antibody using primary myotubes following infection with Ad-PPAR β or Ad-GFP control. (Top) Schematic shows the location of PCR primer sets used to scan the *Ldhb* gene promoter. (Bottom) Graph displays mean (\pm SEM) SYBR green quantification of ChIP normalized to the value for the IgG control (= 1.0). $*P < 0.05$ compared to GFP IgG control.

Supplemental Figure 5. Differential expression of the *Mef2* genes in MCK-PPAR β versus MCK-PPAR α muscle. Expression of the genes encoding MEF2 transcription factors (qRT-PCR) in gastrocnemius muscle compared to NTG control (n \geq 8 mice in each group). Values represent mean (\pm SEM), and shown as arbitrary units (AU) normalized (=1.0) to the value of NTG control. * P < 0.05 vs NTG.

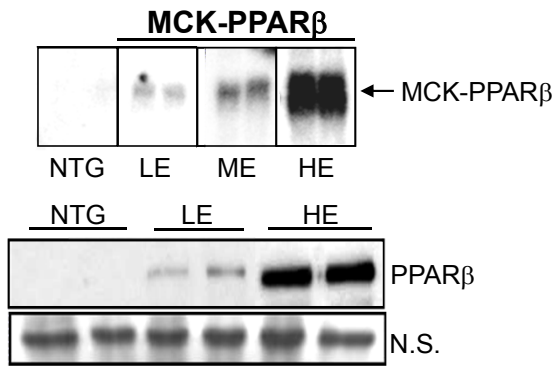
Supplemental Figure 6. Increased mitochondrial biogenesis and fatty acid oxidation capacity in PPAR transgenic mice. (A) Representative electron micrographs of soleus muscle (n=5 per group) showing subsarcolemmal mitochondria in sections from MCK-PPAR mice and corresponding non-transgenic (NTG) littermates. (B) Results of quantitative PCR to determine mitochondrial DNA levels in soleus muscle of the indicated genotypes (n \geq 5 mice per group) using primers for NADH dehydrogenase (*Nd1*, mitochondria-encoded) and lipoprotein lipase (*Lpl*, nuclear-encoded). *Nd1* levels were normalized to *Lpl* DNA content and expressed relative to NTG (=1.0) muscle. Results are expressed as mean \pm SEM. (C) Respiration rates determined from mitochondria isolated from hindlimb muscle of indicated genotypes using palmitoylcarnitine as substrate. ADP-dependent respiration (state 3), oligomycin-induced state 4 (oligo) and the respiratory control ratio (RC) are shown. * P <0.05 vs NTG.

Supplemental Figure 7. Stimulation of mitochondrial respiration by increased LDHB/LDHA ratio is pyruvate-dependent. OCR in primary mouse myotubes transfected with *Ldha* or control siRNAs. OCR was measured without sodium pyruvate for Basal, with 2 μ M oligomycin (Oligo; to inhibit ATP synthase) and after the addition

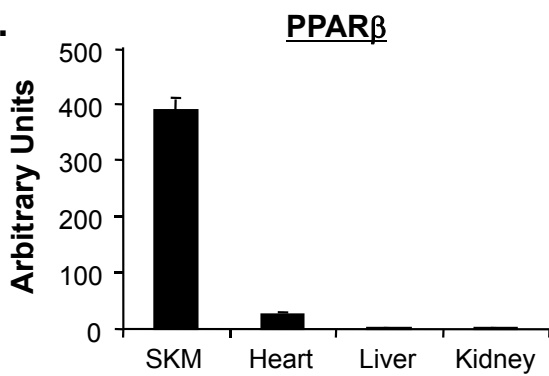
of the uncoupler FCCP (2 μ M). Thereafter, 10 mM sodium pyruvate (Pyruvate) was added. Values represent mean (\pm SEM), n = 3 separate experiments done in 5 biological replicates. * P < 0.05 vs. control.

Supplemental Figure 8. MCK-PPAR β mice maintain high RER despite high oxygen consumption during exercise. (A) Respiratory exchange ratio (RER) during a graded exercise regimen as described in Materials and Methods. (B) VO_2 (oxygen consumption) and (C) ΔVO_2 (increase in oxygen consumption) during an exercise bout in MCK-PPAR β and NTG mice. The grey shaded area in the VO_2 and ΔVO_2 line graphs illustrate the difference in time to exhaustion in MCK-PPAR β mice (1335 ± 134 sec) compared to NTG controls (846 ± 162 sec). Peak VO_2 ($\text{VO}_{2\text{max}}$) and Peak ΔVO_2 are graphed on the right in (B) and (C) respectively. Values represent mean (\pm SEM), n = 5-6 mice in each group. * P < 0.05 vs. NTG.

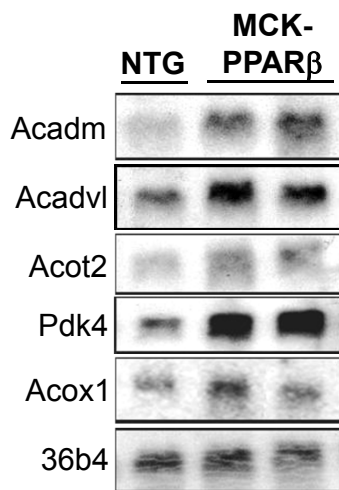
A.



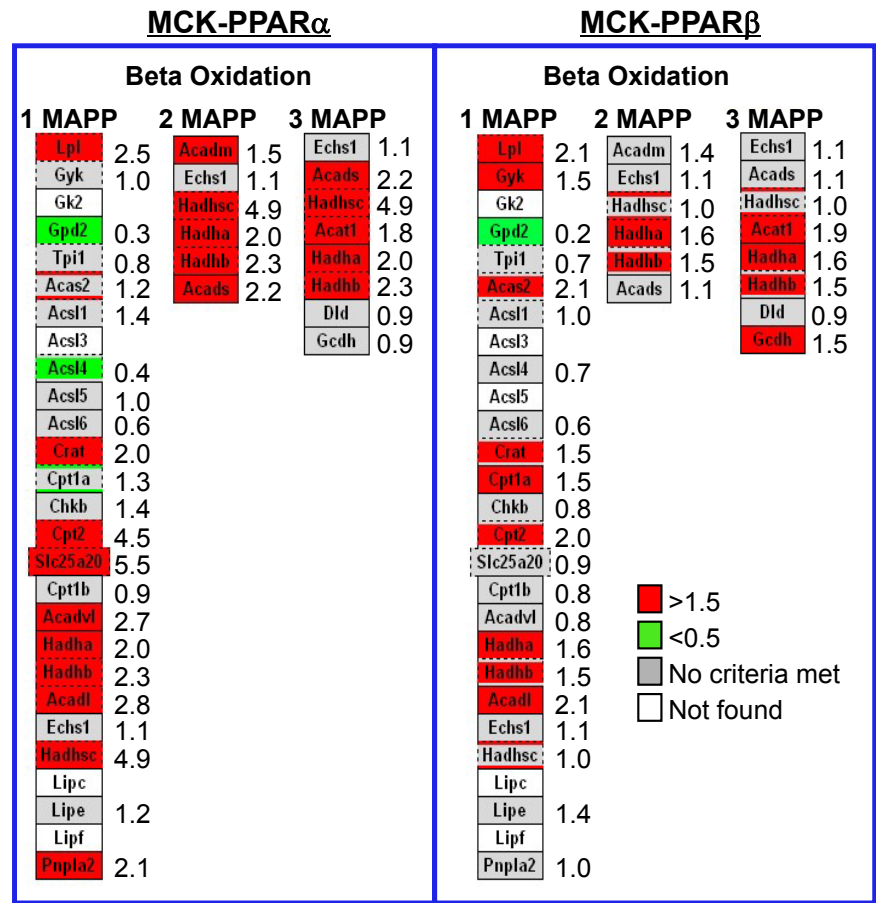
B.



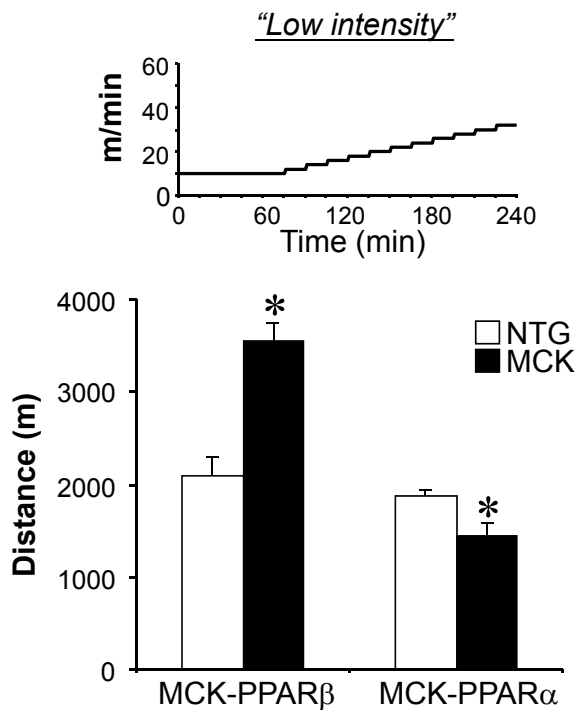
D.



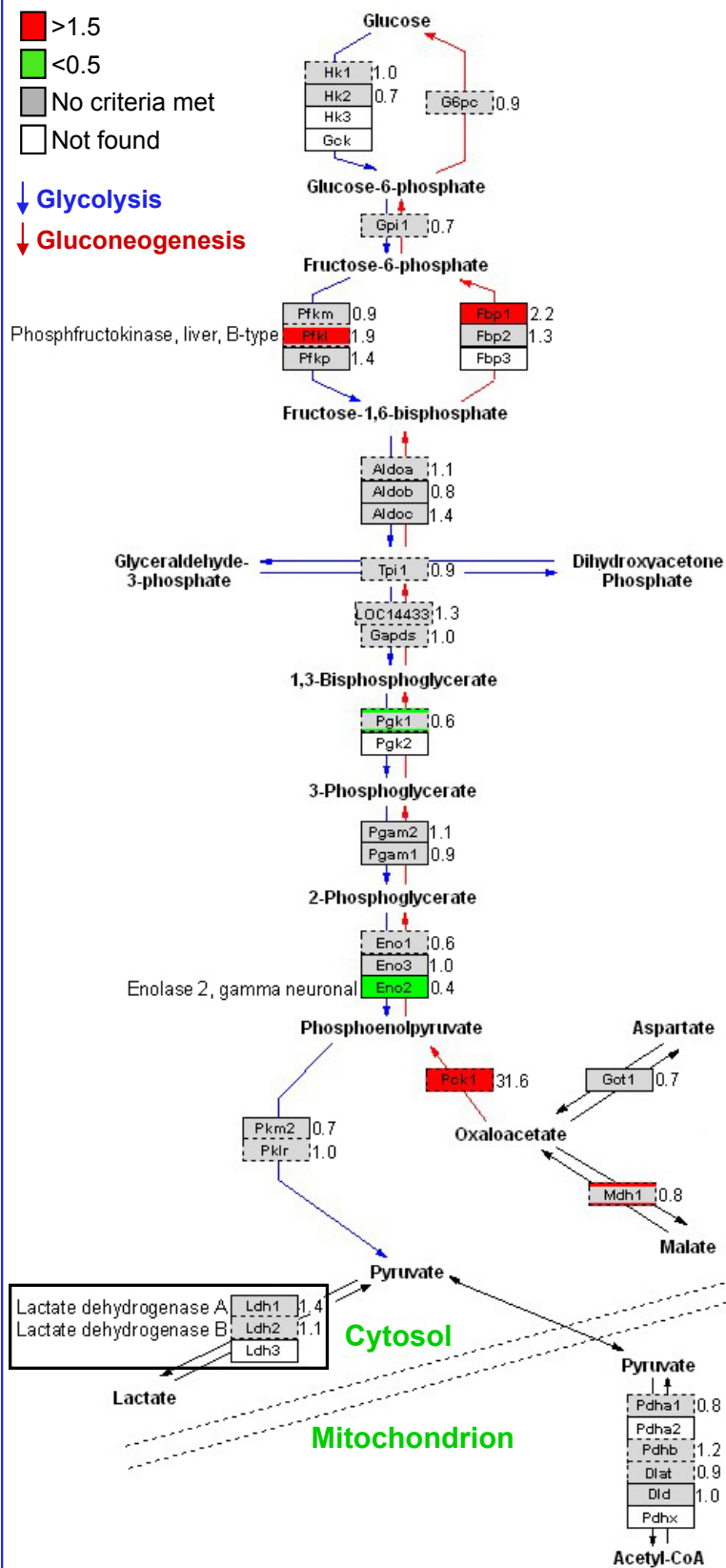
C.



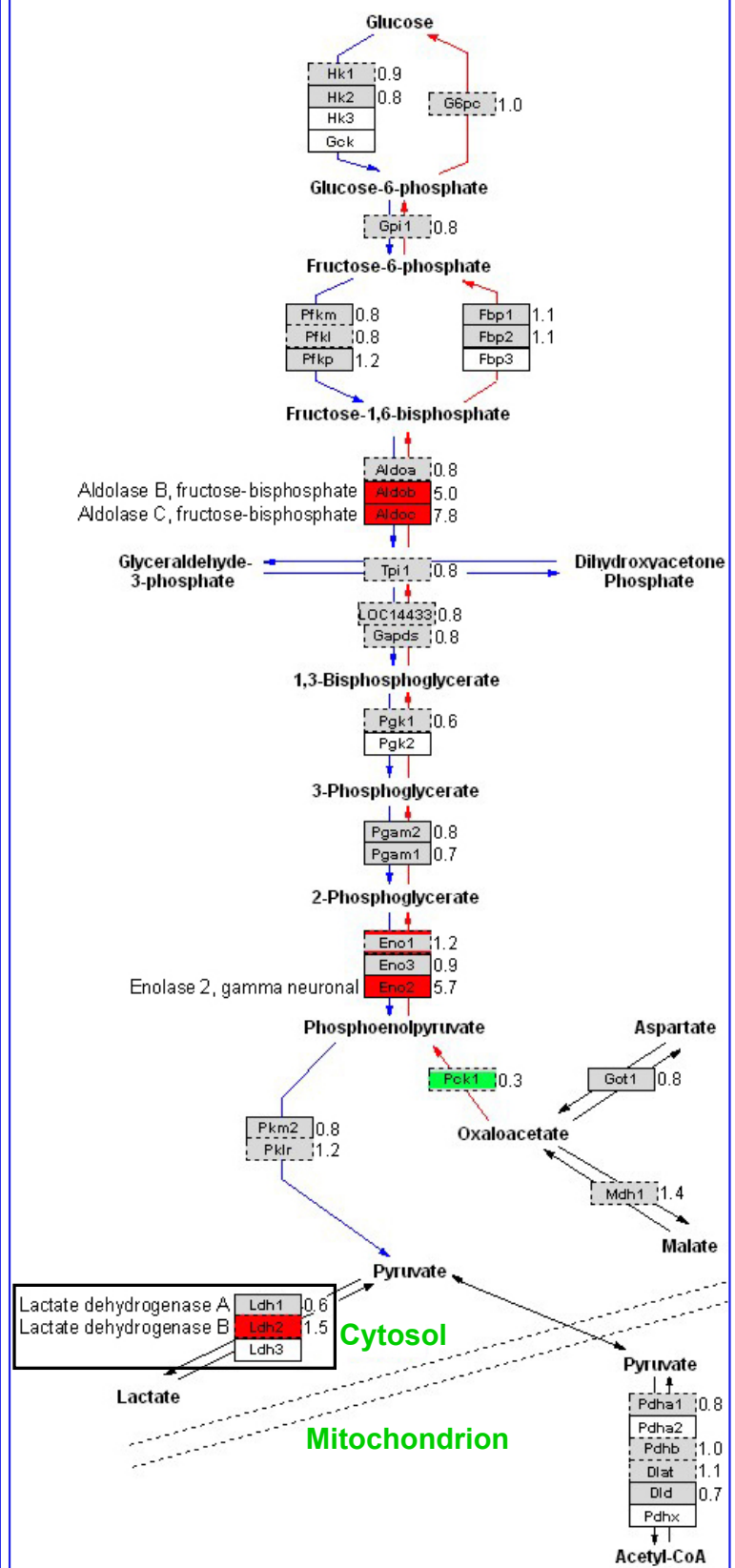
E.

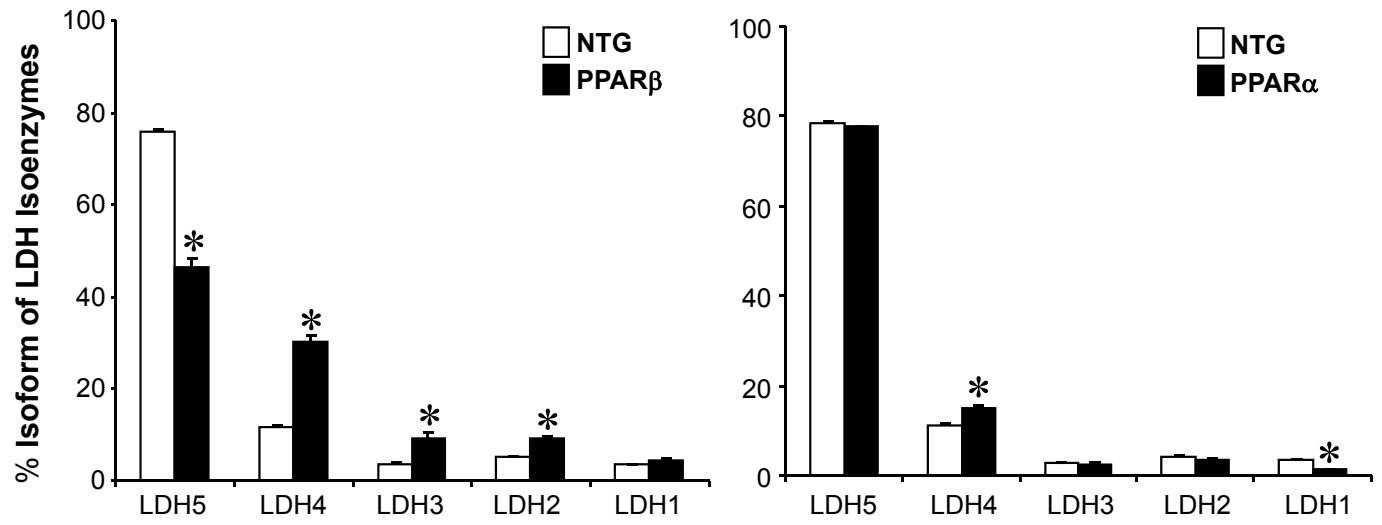


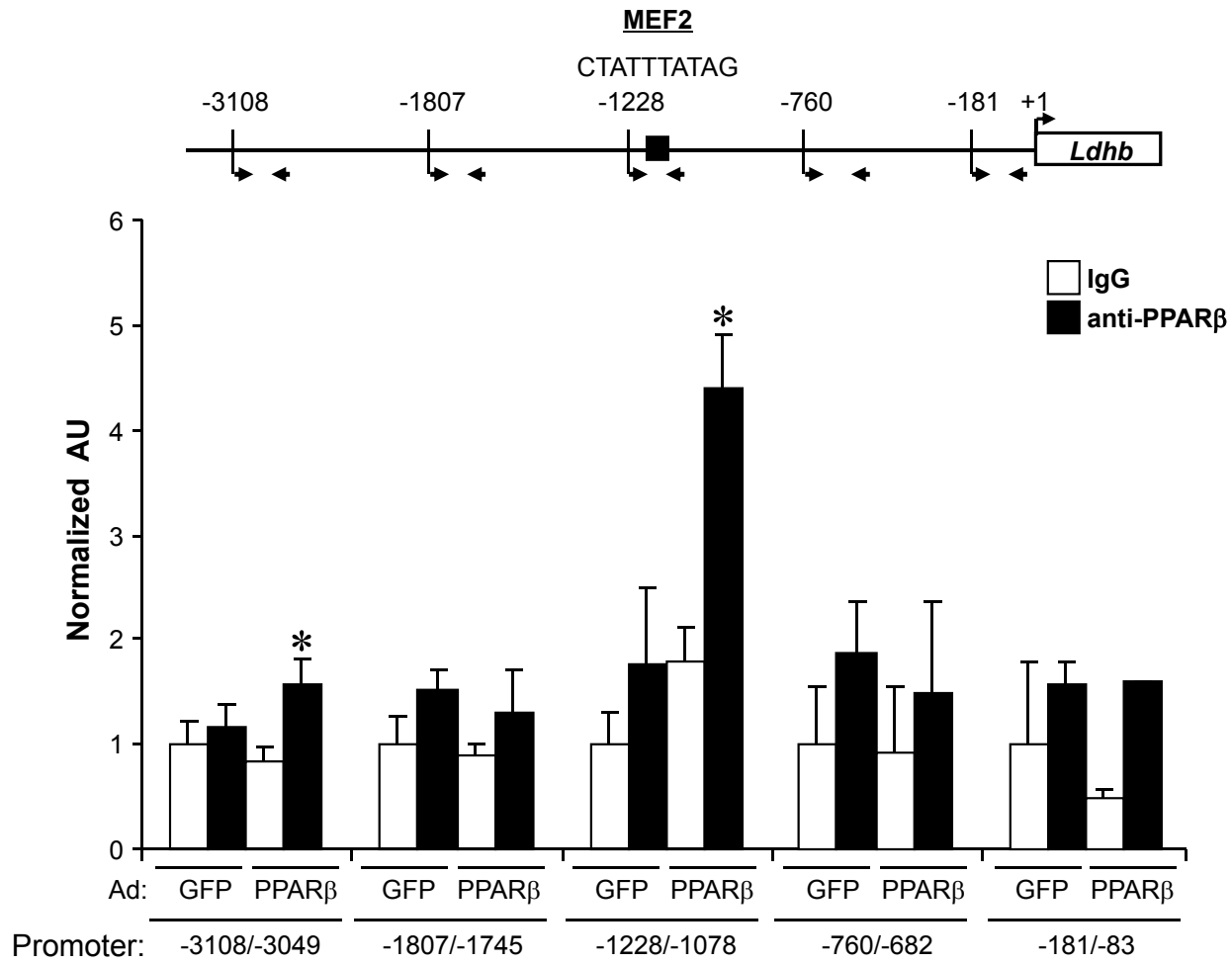
MCK-PPAR α



MCK-PPAR β







A.